Proceedings of the 2001 IEEE
International Conference on Robotics & Automation
Seoul, Korea - May 21-26, 2001

COMPLIANT GRASPING FORCE MODELING FOR HANDLING OF LIVE OBJECTS

Kok-Meng Lee, Jeffry Joni, and Xuecheng Yin
The George W. Woodruff School of Mechanical Engineering,
Georgia Institute of Technology
Atlanta, GA 30332-0405

ABSTRACT

This paper models quasi-statically the force acting on an object by a rotating flexible finger. As compared to fingers with multiple active joints, flexible fingers have many potential advantages; specifically, they are lightweight and have no relative individual moving parts in each of the fingers. Their ability to accommodate a limited range of varying sizes, shapes, and the natural reactions of some objects (without the need of a feedback mechanism such as a visual servo) makes a system using flexible fingers an attractive candidate for use as a grasper in a high-speed production setting. The advantages of flexible fingers are seldom exploited for grasping, however, because of complicated analyses involved in their design. This paper offers two methods to determine contact points/forces. The first analytical model, based on the Frisch-Fay (1962) flexible bar theory, provides an approximate closed-form solution for determining the contact points and forces. The second method using FEM predicts the stress distribution around the contact area. Both methods of predicting the contact forces have been verified experimentally. The effects of parameter variations are presented. Our results demonstrate that the model could be used as a practical means to measure the contact force between the finger and the live object.

1. INTRODUCTION

Many industries that process natural products require transfer of live objects from conveyors to moving processing lines. One of the challenges in prototyping an automated live-object transfer machine is to address the problem of grasping the natural moving object without causing damage or stress, while also meeting the production throughput requirement at a reasonable cost.

Grasping has been addressed extensively in the literature in the past two decades. However, most robotic grasping research has assumed knowledge of object's shape, location, and orientation. Once exact object information is established, finger positions that ensure force-closure grasp are designated. Live, natural objects, however, are typically characterized by varying sizes and shapes in batch processing, and they have natural reflexes (or voluntary motion); consequently the exact position and shape are not known *a priori*. Although some research efforts have recently been directed towards grasping an unknown object, most of these papers assume that the object being grasped is rigid, and that the multi-joint fingers are typically composed of multiple, rigid members. For high-speed automated transfer of live objects from conveyors to moving processing lines, it is often necessary to "grasp" the object in continuous motion in order to minimize the object's natural response variability and struggle. In addition, grasping must be performed with relatively soft fingers to avoid bruising the objects.

Rotating rubber fingers have been used in poultry harvesters to drive broilers into cages for transportation from farms to processing plants (Kettlewell and Turner, 1985). Unlike the poultry harvester; however, transferring a live bird onto a moving shackle at a poultry processing plant requires each of the birds to be manipulated to allow both legs of the bird to be located. Figure 1 shows a CAD model of the compliant grasper, consisting of a pair of rollers, each having n columns of evenly spaced rubber fingers. The two rollers (driven by a servomotor) rotate at the same speed but in opposite directions. Such rotating fingers could be used to singulate live broilers on a conveyor for subsequent handling (Lee *et al.* 1999). Other potentially useful applications include rejecting cadavers from the feed, sorting, and re-orienting the singulated objects (Lee, 1999) and transfer of live broilers to shackles (Lee, 2000).

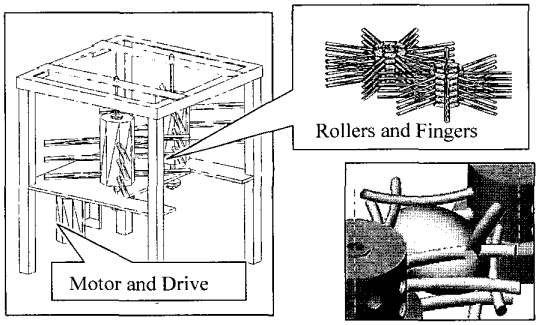

Figure 1 CAD models of a compliant grasper

Flexible fingers have no relative individual moving parts, no backlash, no mechanical noises and no lubrication. These inexpensive fingers can be easily manufactured, assembled and replaced. The advantages of flexible fingers are seldom exploited for grasping, however, because their design involves complicated analyses. The location-dependent force in grasping, coupled with the effect of energy storage in the flexible members and the non-linearity introduced by the large deflection, complicates the modeling and analysis. Furthermore, the exact composition of the rubber used is usually proprietary and mechanical properties of the fingers are not available. Due to these difficulties, the design of flexible fingers has been accomplished by extensive trial-and-error methods. The ability to predict the contact forces and stresses experienced by the object during grasping could offer a more cost-effective design of a grasper. By assuming the deflected finger to have the form of a parabolic function, Lee *et al.* (1999) decoupled the computation of the contact point from the contact force, making the problem more tractable. Our earlier approach that provides a good initial estimate, however, does not account for the frictional effect at the contact interface.

0-7803-6475-9/01/$10.00© 2001 IEEE

Commercial broilers (5-8weeks of age) often do not have fully grown feathers and thus, a limited range of contact surfaces (skins/feathers) must be considered. In this paper, we offer the following:

(1) A quasi-static model to predict the contact force acting on a moving object by a rotating flexible finger:

Unlike the method presented in (Lee, 1999), the quasi-static model described here does not assume the form of the deflected finger and does consider the frictional effect at the contact interface. The model has been verified experimentally and compared to those obtained by an off-the-shelf finite-element code (ANSYS) capable of large deflection analysis. It is expected that the quasi-static model can be extended to a system with multiple fingers.

(2) It provides a force prediction algorithm to analyze the effects of the design parameters on the grasping force:

The effect of the stiffness on grasping forces has been examined analytically and experimentally using two different types of rubber fingers and two different values of object stiffness; the results agree well with the conclusions reached analytically. Two methods are used to analyze the effects of stiffness on the contact forces. The first method, based on the Frisch-Fay (1962) flexible bar theory, provides an approximate closed-form solution for determining the force at the contact point. The second method uses FEM to predict the stress distribution around the contact area. Both prediction methods have been verified experimentally.

(3) It offers a practical way to measure the contact force acting on a live object such as a broiler:

The bird's feathers often make direct measurements of the contact force (with photo-stress or pressure sensors) nearly impossible. As will be discussed, our model provides a basis for experimentally measuring of the contact force from the shape of the deflected finger, which can be obtained from machine vision images. These research results have immediate applications in the poultry industry where a system automating the transfer of live birds is preferred over the expensive/unpleasant manual operation.

2. MODEL OF A ROTATING FLEXIBLE FINGER

Figure 2 shows the coordinate systems describing the kinematics of a rotating finger acting on an object, where XYZ is the fixed (reference) coordinate frame assigned at the center of a rotating cylinder with its Z-axis along its rotating axis; x_cy_c is the coordinate frame attached on the object; and x_fy_f is a moving coordinate frame attached at the base of the finger. When the rotating finger is in contact with an object, the reaction force f causes the finger to deflect. The contact point on the finger is described with respect to the XYZ frame by

$$\mathbf{X}_i = \mathbf{T}(\phi)\,\mathbf{x}_i + \mathbf{X}_r \tag{1}$$

where

$$\mathbf{X}_r = [r\cos\phi,\ r\sin\phi]^T; \tag{2}$$

$\mathbf{T}(\phi) = \begin{bmatrix} \cos\phi & -\sin\phi \\ \sin\phi & \cos\phi \end{bmatrix}$; $\phi(t) = 2\pi - \omega t$; and ω is the angular speed and r is the radius of the roller. Similarly, since the object shares the same contact point, we have

$$\mathbf{X}_i = \mathbf{T}(\theta)\,\mathbf{x}_{ci} + \mathbf{X}_o \tag{3}$$

where θ is the orientation of the x_cy_c coordinate frame; and $\mathbf{X}_o = [vt + X_o \quad Y_o]^T$; v is the conveyor (and hence, the linear speed of the object); X_o is the initial object position in the X direction. From Equations (1) and (3),

$$\boldsymbol{x}_i = \mathbf{T}^{-1}(\phi)\,\mathbf{T}(\theta)\,\mathbf{x}_{ci} + \mathbf{T}^{-1}(\phi)(\mathbf{X}_o - \mathbf{X}_r) \tag{4}$$

The rotating finger is treated as "quasi-static" and the equations are solved approximately using static mechanics. In this case, the equations of static mechanics can be applied at each instant in time as though the deflected finger were static. The flexible finger can be modeled as a bent elastic rod as shown in Figure 3, where α defines the direction of the contact force acting on the finger; and ψ_o is the slope of finger at the contact point. Since the contact point and the reaction from the object are not known *a priori* in grasping, five unknowns, x_i, y_i, ψ_o, f, and α, have to be solved simultaneously. The deflection of the finger depends on the coefficient of friction at the contact interface, the object geometry, and the shape of the deflected finger.

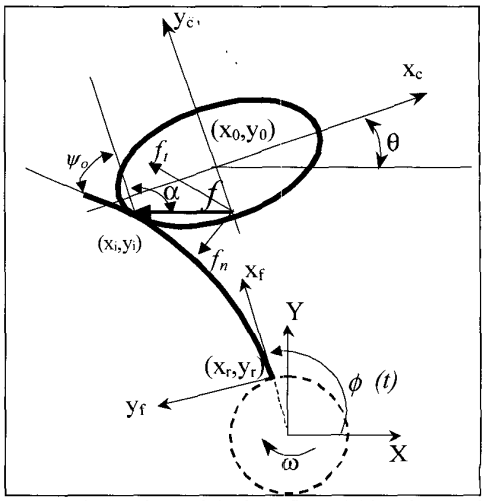

Figure 2 Kinematic model of the finger/object interaction

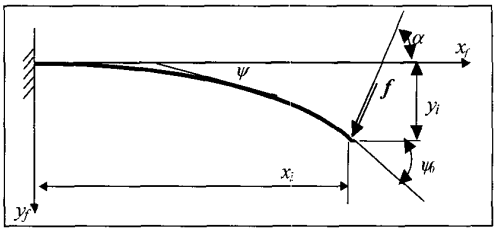

Figure 3 Model of a bent flexible finger

Contact interface

In quasi-static equilibrium, we have

$$\mu = \frac{f_t}{f_n} = \tan(\alpha + \psi_o - \frac{\pi}{2}); \tag{5}$$

where μ is the coefficient of friction between the finger and the object; and the subscripts t and n denote the tangential and normal components of the contact force perpendicular to and along the finger at the contact point respectively.

Object geometry

The location and the slope of the object at the contact point

must satisfy the following equations:

$$f_o(x = x_i, y = y_i) = 0 \tag{6a}$$

$$\left.\frac{\frac{\partial f_o(x,y)}{\partial y}}{\frac{\partial f_o(x,y)}{\partial x}}\right|_{(x=x_i, y=y_i)} = \tan\psi_o \tag{6b}$$

where $f_o(x, y) = 0$ describes the geometry of the object.

Deflection of a flexible finger

For a given force vector $\boldsymbol{f}$ exerted at a known location, the deflected shape of the finger can be described using Equations (7a) and (7b) with ψ as a parameter (Frisch and Fay, 1962):

$$x = \frac{1}{k}\left[2p\sin\alpha(\cos\varsigma - \cos\xi) - h(\psi_o)\cos\alpha\right] \tag{7a}$$

$$y = \frac{1}{k}\left[2p\cos\alpha(\cos\varsigma - \cos\xi) + h(\psi_o)\sin\alpha\right] \tag{7b}$$

where $h(\psi) = [F(p,\xi) - F(p,\zeta) - 2E(p,\xi) + 2E(p,\zeta)]$ (8a)

$$p = \sin[(\psi_o + \alpha)/2]; \tag{8b}$$

$$\varsigma = \sin^{-1}\left[\frac{\sin(\alpha/2)}{p}\right]; \quad \xi = \sin^{-1}\left[\frac{\sin[(\psi+\alpha)/2]}{p}\right] \tag{8c}$$

$$k = \sqrt{\frac{|f|}{EI}}; \tag{9}$$

and where E is the Young's modulus; I is the moment of inertia of the finger; and $F(p,\varsigma)$ and $E(p,\varsigma)$ are the standard form of elliptical integrals of the first and second kinds respectively.

The deflection at the contact point can be determined by noting that $\psi = \psi_o$ and thus $\xi = \pi/2$. Equations (5), (6a), (6b), (7a), and (7b) provide the necessary equations to solve the five unknowns, x_i, y_i, ψ_o, k, and α. The reaction force f can then be computed from Equation (9). The flowchart illustrating the computing procedure is given in Figure 4.

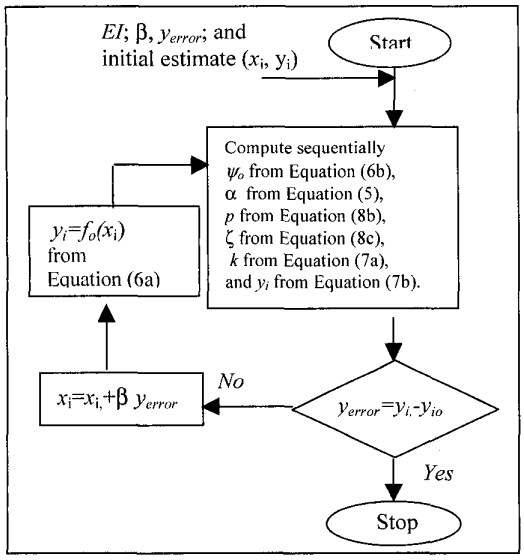

Figure 4 Flowchart illustrating the computational procedure

3. CONTACT FORCE PREDICTION ALGORITHM

In order to have a better understanding of the effects of the rotating fingers on an object on a moving conveyor, a simulation program has been written to locate the contact point, and to predict the magnitude of the contact force; these variables are important for predicting any potential bruises on the live object. We model the broiler as an ellipsoid and the fingers are treated as flexible bars as discussed in (Lee, 1999). For clarity, we present the simulation based on a single rotating finger on a two-dimensional ellipse (Figure 2) that characterizes the cross-section of the broiler in the plane of rotating finger.

Finger properties

An 8-inch (203.2mm) long finger manufactured by the Waukesha Rubber Company, as shown in Table 1, was chosen in this application. The finger is flexible in the XY plane in order to adapt for the size variation but is relatively rigid in the Z direction in order to support the static weight of the broiler. The finger properties are summarized in Table 1.

Table 1: Finger properties

Parameters	Values
Mass	0.079 kg
Density	1023.43 kg/m^3
Major radius, a	12 mm
Minor radius, b	8.45 mm

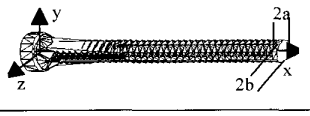

Figure 5 shows an experimental setup for determining the effective EI of the finger, where a known force f is applied perpendicular to the x-axis (i.e., $\alpha = \pi/2$) at a known location on the finger. Equation (7b) can be written in the following form:

$$[C(\psi_o)]^2 = EI[h(\psi_o)]^2 \tag{10}$$

where

$$C(\psi_o) = y_f\sqrt{f} \tag{11}$$

The effective EI is essentially the slope of the curve where $C^2(\psi_o)$ is plotted against the function $h^2(\psi_o)$ computable from Equation (8a). By measuring the deflection and the slope at the contact point ($y = y_f$ and $\psi = \psi_o$), the relationships between $C^2(\psi_o)$ and $h^2(\psi_o)$ were obtained experimentally for two different finger types (WK52E and WK52H) that have an identical geometry but different compositions. The values of the effective EI_z for the WK52E and WK52H rubber fingers were determined experimentally to be 0.08Nm^2 and 0.169Nm^2 respectively.

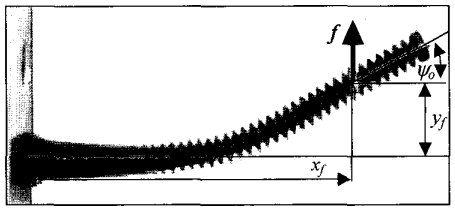

Figure 5 The finger's properties are obtained experimentally

Quasi-static motion simulation

The values of the parameters used in the simulation are given in Table 2. The y_{error} value was chosen to be 0.001m or less. The range of β was tested computationally for convergence, and the appropriate range of values for β was found to be from 0.01 to 0.3. We notice that if β is more than 0.5, the recursive method may not converge. When the slope is near infinity (or the tangent line at the contact point becomes vertical), the algorithm would oscillate at that point. To avoid this problem, we decrease the step size or the coefficient β, and when the slope is approaching infinity, the x_{error} is used as a criterion of convergence.

Table 2: Simulation parameters and values

Simulation Parameters	Values
Bird's half width along major axis	0.1 m (3.9inches)
Bird's half width along minor axis	0.067m (2.65 inches)
Initial Location of the ellipse,	X_o=-0.332m (-13 inches), Y_o=0.184m (7.25 inches), $\theta = 0°$
Initial angular position of finger	ωt=180°
Length of finger	0.203m (8 inches)
Radius of the roller	r = 0.0762m (3 inches)
Coefficient of friction	0.4104
EI of the rubber finger	0.08 Nm^2
Conveyor speed	0.508m/s, 20 inches/second
Angular speed of rollers	20 rpm

Figure 6 shows the simulated trajectory of a broiler on the conveyor as the flexible finger exerts on the broiler. Quantitative data that characterizes the contact are given in Table 3, which shows that the maximum force acting on the broiler is in the order of 25N. The four sets of data (shaded, between 72° and 126°) will be used as a basis for comparison in the following sections.

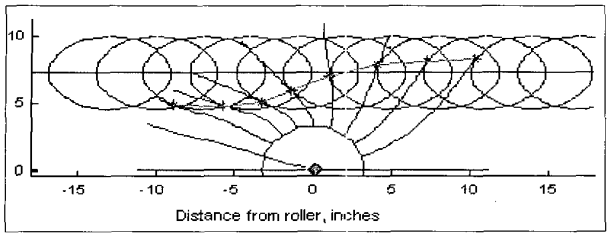

Figure 6 Simulation of the rotating finger

Table 3: Simulated values describing the deflected finger

ϕ (°)	x_i (m)	y_i (m)	ψ_o(°)	| f | (N)	α (°)
144	0.1731	0.032	15.7	1.685	105.26
126	0.1029	0.046	35.6	8.77	85.39
108	0.0662	0.040	46.1	23.365	74.88
90	0.0673	0.035	41.1	21.885	79.87
72	0.0959	0.029	25.2	8.055	95.78
54	0.1401	0.031	18.8	2.975	102.17
36	0.1901	0.059	25.7	2.08	95.30
18	0.234	0.119	40.0	1.795	80.92

4. VERIFICATION OF THE ANALYTICAL MODEL

The analytical results have been verified experimentally, and are also compared to those obtained by an off-the-shelf finite-element code (ANSYS) capable of large deflection analysis. The objectives of the experiments are (1) to examine the "quasi-static" assumption, and (2) to serve as basis for comparing the two analytical methods for predicting forces.

4.1 Experimental Results

To verify the analytical model, an aluminum elliptical cylinder (25mm height) was fabricated as a model representation of a bird in the plane of the rotating finger. The coefficient of friction at the rubber-aluminum interface was determined experimentally to be μ=0.6041. Other parameters used in the experiment are given in Table 2. The elliptical object was mounted on a 6-DOF-force/torque transducer (Mini US 20/40 manufactured by ATI Industrial Automation) to deduce the force/torque at the contact between the finger and elliptical object. The object position was fixed at specific positions from the drum center. At each position, the force/torque data as a function of time were acquired as the drum rotates at a specified speed, and the contact forces between the finger and the object were then computed from the equations of static mechanics.

The forces on the object (moving along Y_o=0.184m or 7.25 inches at θ = 0°) were measured for a range of angular speeds typically used in dynamics grasping. Figure 7 shows a sample plot of force trajectory obtained experimentally. Figure 7(a) shows the measured forces as a function of the finger's angular position for five different values of X_o at a constant speed of 20rpm. Figure 7(b), which graphs the measured forces on the object at $X_o = -25mm$ for five different angular speeds (15, 20, 22, 24, 25rpm), shows the finger dynamics do not have significant effects on the contact forces for the range of speeds up to 25rpm. The similarity in the force curve suggests that for a relatively slow, constant drum speed, the force acting on the object is primarily a function of the finger deflection and that the contact mechanics can be determined quasi-statically.

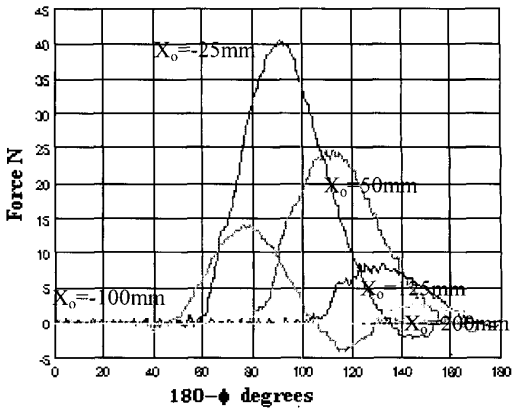

(a) 5 different X_o at a constant speed of 20rpm

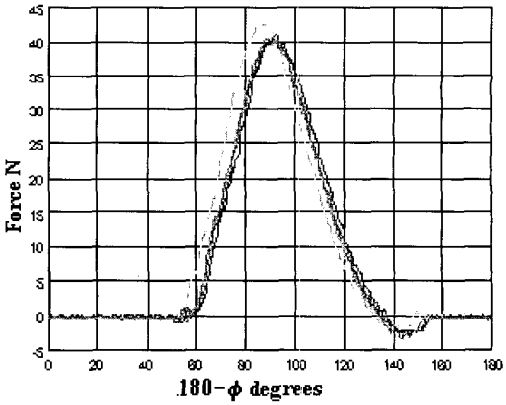

(b) 5 different angular speeds at $X_o = -25mm$

Figure 7 Experimentally measured forces

4.2 Finite Element Method (FEM)

As in the Frisch-Fay flexible bar theory, the FEM model is also based on the Bernoulli-Euler beam theory that considers a large deflection analysis on the model. However, the FEM allows an area contact to be applied to the finger model, and accounts for the varying geometrical cross-section of the rubber finger by discretizing it into several smaller beam elements. It also predicts the stress distribution that provides a means to locate (and thus

prevent) potential bruises due to grasping.

Using ANSYS, the finger is modeled as a 2D elastic beam element (Beam3), which is a uni-axial element with tension, compression, and bending capabilities. The element has 3 DOF at each node, translations in the nodal x-and y-directions and a rotation about the nodal z-axis. It has a large deflection analysis capability and the transverse shear strain is not zero. With the ability to model the finger in a non-uniform cross-section in FEM, the Young's modulus can be obtained specifically by computing iteratively such that the forces applied would result in the deflections obtained in the experiment as shown in Figure 5. The Young's moduli for the WK52E and WK52H have been determined to be E_e = 4.2MPa and E_h = 6.31MPa respectively.

In the FEM analysis, the ellipse is fixed and the relative displacements are applied as constraints at the base of the finger as a function of time with respect to the ellipse coordinate frame as shown in Figure 8. The element type Plane42 was used in ANSYS for the ellipse, which is a 4-node quadrilateral structural solid with two transverse (x-axis and y-axis) DOF. A 200 time load steps was chosen with 100 sub-steps for each load step with the limit of a 10,000 maximum and 10 minimum sub steps. Results are summarized in subsection 4.3.

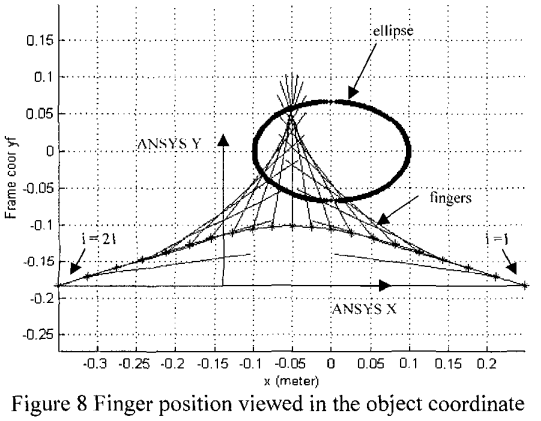

Figure 8 Finger position viewed in the object coordinate

4.3 Comparison of Quasi-static Force Prediction

The results of the analytical model and the FEM are compared against the experimental data for the motion trajectory shown in Figure 6, where the values of the parameters and the simulated results have been given in Tables 2 and 3 respectively, and the experimental data were determined from Figure 7.

Figure 9 compares the computed shape of the deflected finger against the shape found in the images captured experimentally for four different instants highlighted (shaded in gray) in Table 3. Figure 10 shows the stress contours at the corresponding contact points. The resultant forces, simulated using both methods, are compared against the experimental data in Figure 11. The comparisons show that the analytical model provides a reasonable prediction of the contact points and forces.

5. EFFECTS OF PARAMETER VARIATION

As discussed in Section 2, the resultant contact forces depend on EI, μ, object geometry as well as the instantaneous position of the finger with respect to the object arrival.

Lee *et al.* (2000) conducted a meat coloration examination at the University of Georgia to determine any bruises that might be caused by the flexible fingers. Using a Minolta Colorimeter, they evaluated 4 different trials of 6 birds each, providing a means to compare two groups of birds (female and male) subjected to the rotating fingers (WK52E) at 20rpm against the respective (control) groups of birds transported through the same conveyor but without rotating fingers. Their results found no significant differences among the 4 trials. To provide a better understanding, we stimulate the effect of the object stiffness on contact forces using two different material properties: aluminum (E_a =7.31Gpa) simulating bone, and silicone (E_s =0.1Mpa) simulating meat.

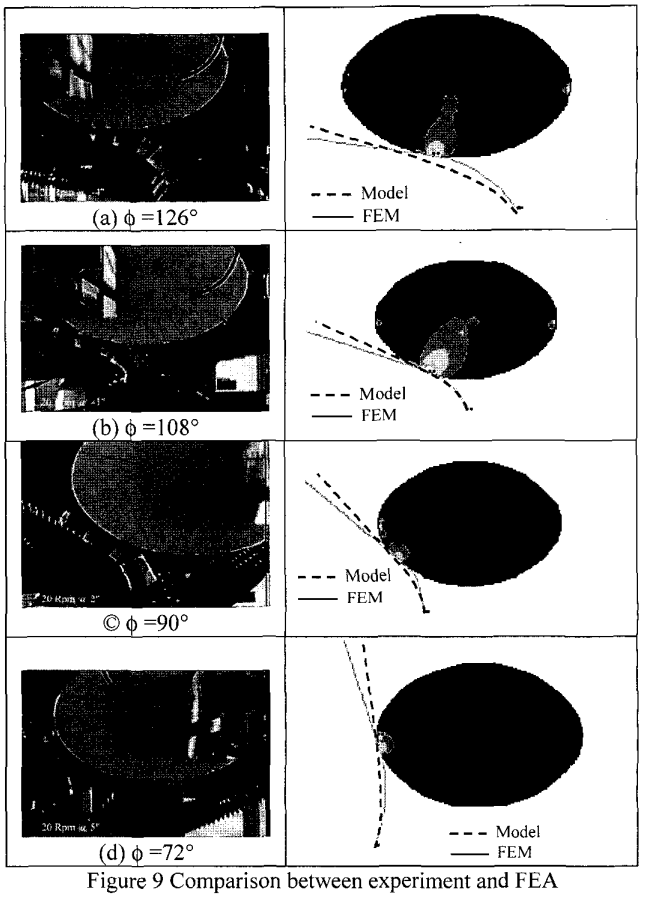

Figure 9 Comparison between experiment and FEA

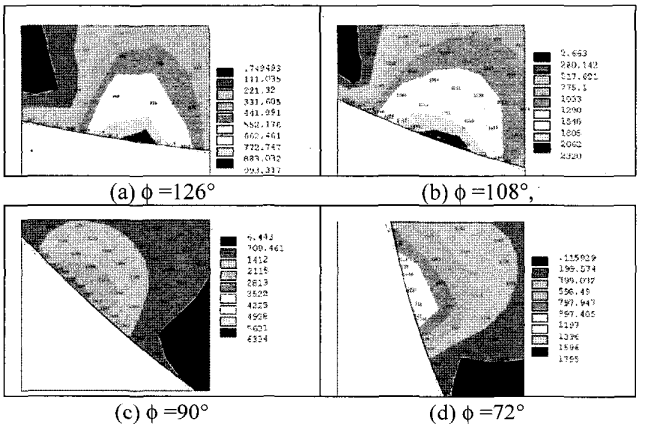

Figure 10 Stress Contours (Stress in Pa)

Tables 4 and 5 tabulate the maximum stress and contact force respectively for each of the constraint conditions based on the color information of the FEM results. The maximum stresses for type E and H fingers with the aluminum ellipse are on average of 7.38% and 8.13% respectively higher than that with the silicone ellipse. *No significant differences are observed in resultant contact forces between the two types of object stiffness.* These results agree with those obtained from the coloration test.

However, the maximum stresses for WK52H finger is an average of 49.73% higher than that for WK52E for the same object. As compared in Table 4, the difference in the maximum stresses due to the different object stiffness (E_a/E_s = 7,310) is six times smaller than that due to the finger stiffness (E_h/E_e = 1.5). The results indicate that *the flexural rigidity of the fingers, EI, plays an important role in governing the contact force* and thus, in predicting the potential bruising of the birds due to the fingers.

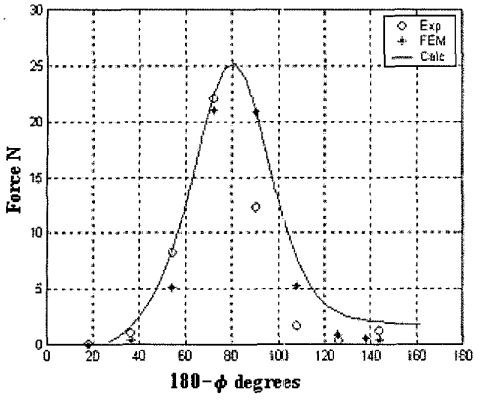

Figure 11 Comparison of results

Table 4: Maximum stress

	Max Stress (Pa)			
ϕ(°)	WK52E		WK52H	
	E_a =7.31 GPa,	E_s = 0.1 MPa	E_a = 7.31 GPa	E_s = 0.1 MPa
126°	993	893	1440	1260
108°	2320	1958	3485	2936
90°	3522	3435	5409	5320
72°	1596	1574	2397	2334

Table 5: Reaction forces

	Reaction Force (f_r) (N)			
ϕ(°)	WK52E		WK52H	
	E_a =7.31 GPa,	E_s = 0.1 MPa	E_a = 7.31 GPa	E_s = 0.1 MPa
126°	5.10	5.07	7.66	7.57
108°	21.33	20.31	31.80	30.17
90°	20.66	20.18	30.71	30.79
72°	5.26	5.19	7.72	7.71

The analytical model can be used as an aid to measure the contact force of a live broiler. Figures 12(a) and 12(b) show contact force measurements performed on two different types of birds; generically grown birds without feathers and a bird will full grown feathers. In each case, video images of the deflected finger were obtained as the finger acted on the bird, and the contact forces were then computed iteratively such that the forces applied would result in the deflections obtained experimentally as shown in Figure 12(c) for a given bird size and contact point. Figure 12(d) shows that *the contact forces increase with the coefficient of friction*, which simulates the finger acting on a bird of 0.138m (5.5in.) wide starting with an initial X_o =-0.483m (-19 inches). The comparison between Figure 12 and Figure 11 where X_o =-0.332m (-13 in.) shows that *the motion synchronization of the finger with respect to the arrival of the bird has a significant effect on the magnitude of the contact force acting on the object.*

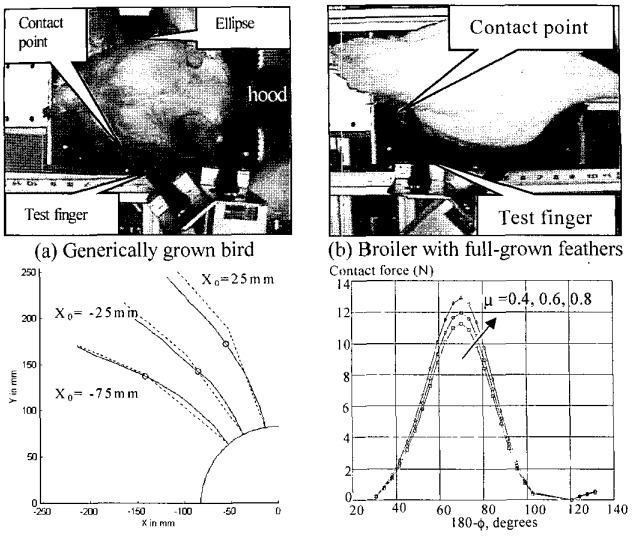

(a) Generically grown bird (b) Broiler with full-grown feathers

(c) Deflection of finger (d) Effect of μ (0.4, 0.6, 0.8)

Figure 12 Force measurements of live birds

6. CONCLUSIONS

A quasi-static model for predicting the force acting on a moving object by a rotating finger has been presented. Two methods have been described. The first analytical model, built upon the Frisch-Fay flexible bar theory, provides an approximate closed-form solution for determining the contact points and forces. The second method uses FEM to predict the stress distribution around the contact area. The results of both methods have been verified experimentally using two different types of rubber fingers, and results agree well with the conclusions reached analytically. The effects of the design parameters on the forces and stresses at the contact area have been discussed. The prediction provides a rational basis for design optimization and force measurement of a grasper using flexible rotating fingers. Future studies include the effects of stresses on potential bruises.

ACKNOWLEDGEMENT

The Georgia Agriculture Technology Research Program and the US Poultry and Eggs Association have jointly funded this project. We thank Dr. Jeff Buhr of the USDA/ARS for arranging a generic bird.

REFERENCES

1. Frisch-Fay, R., 1962, "Flexible Bars," Washington, Butterworths.
2. Kettlewell, P. J. and M. J. Turner, 1985, "A Review of Broiler Chicken Catching and Transport Systems," Journal of Agricultural Engineering Research, 31, pp.93-114.
3. Lee, K.-M., 1999, "On the Development of a Compliant Grasping Mechanism for On-line Handling of Live Objects, Part I: Analytical Model," AIM'99, Atlanta, GA, Sept. 19-23.
4. Lee, K.-M. A. B. Webster, J. Joni, X. Yin, R. Carey, M. P. Lacy, R. Gogate, 1999, "On the Development of a Compliant Grasping Mechanism for On-line Handling of Live Objects, Part II: Design and Experimental Investigation," AIM'99, Atlanta, GA, Sept. 19-23.
5. Lee, K.-M., 2000, "Design Criteria for Developing an Automated Live-bird Transfer System," IEEE ICRA'00, San Francisco, Apr. 22-28.
6. Lee, K.-M. R. Carey, A. B. Webster, M. P. Lacy, J. Northcutt, 2000, Intelligent Automated Transfer Of Live Birds To Shackle Line," US P. & E. First Progress Report on Project #446.